Conformational Change of the Rieske [2Fe–2S] Protein in Cytochrome bc_1 Complex

Momi Iwata,[1,2] Joakim Björkman,[1] and So Iwata[1]

Structures of mitochondrial bc_1 complex have been reported based on four different crystal forms by three different groups. In these structures, the extrinsic domain of the Rieske [2Fe–2S] protein, surprisingly, appeared at three different positions: the "c_1" position, where the [2Fe–2S] cluster exists in close proximity to the heme c_1; the "b" position, where the [2Fe–2S] cluster exist in close proximity to the cytochrome b; and the "intermediate" position where the [2Fe–2S] cluster exists in-between "c_1" and "b" positions. The conformational changes between these three positions can be explained by a combination of two rotations; (1) a rotation of the entire extrinsic domain and (2) a relative rotation between the cluster-binding fold and the base fold within the extrinsic domain. The hydroquinone oxidation and the electron bifurcation mechanism at the Q_P binding pocket of the bc_1 complex is well explained using these conformational changes of the Rieske [2Fe–2S] protein.

KEY WORDS: Cytochrome bc_1 complex; cytochrome c reductase; bovine heart mitochondria; Rieske Fe–S protein; protein crystallography; membrane protein.

INTRODUCTION

Cytochrome bc_1 complex (ubiquinol: cytochrome c reductase) is the middle component of the mitochondrial respiratory chain, coupling the transfer of electrons from ubihydroquinone to cytochrome c with the generation of a proton gradient across the mitochondrial membrane. Every bc_1 complex contains three common subunits with active redox centers [cytochrome b, cytochrome c_1, and the "Rieske" [2Fe–2S] protein (ISP)] (Robertson *et al.*, 1993; Yang and Trumpower 1986).

Three different research groups have reported the crystal structures of the bc_1 complex from four different crystal forms. Surprisingly, the ISP extrinsic domain was found to be in different positions. These positions are, in principle, classified into three positions: the "c_1" position, where the [2Fe–2S] cluster

exists in close proximity to the heme c_1; the "b" position, where the [2Fe–2S] cluster exists in close proximity to the cytochrome b; and the "Intermediate" ("*Int*") position, where the [2Fe–2S] cluster exists in-between the "c_1" and "b" positions.

The structure of the bc_1 complex was first reported by Deisenhofer and Yu's group (Xia *et al.*, 1997; Kim *et al.*, 1998). This structure was solved in the $I4_122$ crystal form from the bovine heart bc_1 complex. In this structure, strongly disordered ISP was found to be in the "b" position. Berry's group then produced structures from the chicken bc_1 complex (Zhang *et al.*, 1998; Crofts *et al.*, 1999). They could show the extrinsic domain of the ISP in both the "c_1" position in the native crystals and the "b" position when the protein was cocrystallized with a Q_P site inhibitor stigmatellin. The group of Iwata and Jap determined two new structures of the bovine bc_1 complex in the crystal forms $P6_522$ and $P6_5$ (Iwata *et al.*, 1998). These were the first complete structures of the bc_1 complex but, more surprisingly, the ISP extrinsic domain was found to be in different positions from the bovine $I4_122$ form. The structure from the $P6_522$ crystal form showed the ISP

[1] Department of Biochemistry, Uppsala University, Biomedical Center, Box 576, S-75123, Uppsala, Sweden.
[2] Author to whom all correspondence should be sent.

in the "c_1" position and the $P6_5$ crystal form showed the ISP in the new "Int" postion, in-between the "c_1" and the "b" positions.

These observations show the motion of the ISP extrinsic domain is a critical part of the hydroquinone oxidation and electron bifurcation mechanism at the Q_P binding pocket of the bc_1 complex. However, the mechanisms proposed by the three groups still contain many controversial issues. In this paper, we summarize the ISP motion and try to find the best interpretation of three different forms of the ISP within the mechanistic model of hydroquinone oxidation at the Q_P binding pocket.

CRYSTAL STRUCTURES

Three different crystal structures are used in this paper. For the ISP structures at the "c_1" and the "Int" positions, the crystal structures of our bovine $P6_522$ and $P6_5$ forms were used, respectively (Iwata *et al.*, 1998). Both of the crystals are obtained from naturally oxidized bc_1 complex from bovine heart. The only difference between the two crystal forms was due to the detergent used for crystallization (dodecylmaltoside for the $P6_522$ form and a mixture of dodecylmaltoside and HECAMEG for the $P6_5$ form). The conformational changes between the two crystal forms are due to the differences in crystal packing. In the $P6_522$ crystal form, two ISPs in the bc_1 complex dimer are crystallographically equivalent and, therefore, are in the same conformation ("c_1" form). For the $P6_5$ form, two ISPs are in different conformations: one is in the "Int" form and the other is disordered and a mixture of several discrete forms. The ISPs at the "c_1" position in the $P6_522$ crystal form and the "Int" position in the $P6_5$ form are stabilized by crystal contacts. However, these two positions are not artefactual; both positions are clearly observed in the disordered ISP density in the $P6_5$ crystal form where there is no crystal contact on the ISP. These structures are, in principle, the same as published in the reference (Iwata *et al.*, 1998), however R factors have been improved by further refinement (28.6% for $P6_522$ and 32.5% for $P6_5$). The coordinates have been deposited in the Protein Database (PDB) (1BE3 for $P6_522$, and 1BGY for $P6_5$).

For the ISP structure at "b" position, the crystal structure from the chicken $P2_12_12_1$ form was used (3BCC in PDB). This has been cocrystallized with an inhibitor stigamatellin. In this crystal form, two ISPs

in the dimmer are crystallographically independent and one of the ISP has crystal contact with another bc_1 complex dimer.

An overall view of the bc_1 complex with the ISP in the "c_1" position (bovine $P6_522$ form) viewed parallel to the membrane is presented in Fig. 1. The structures of the bovine $P6_5$ form and the chicken $P2_12_12_1$ form are very similar to this structure except for the conformation of the ISP extrinsic domain. The ISP from one monomer is interacting with cytochrome c_1 and cytochrome b from another monomer and these three subunits are forming a functional unit for the hydroquinone oxidation (thus there are two functional units in the dimer). In the figure, one of these functional units is shown in dark grey. The extrinsic domains of cytochrome c_1 and ISP are positioned on top of cytochrome b. The extrinsic domain of cytochrome c_1 is sitting on helix αab (residues 61–73) and the first half of loop ef (residues 246–261) of cytochrome b. The ISP extrinsic domain ("c_1" position) is located above the other half of loop ef (residues 262–268) of cytochrome b and is also associated with cytochrome c_1
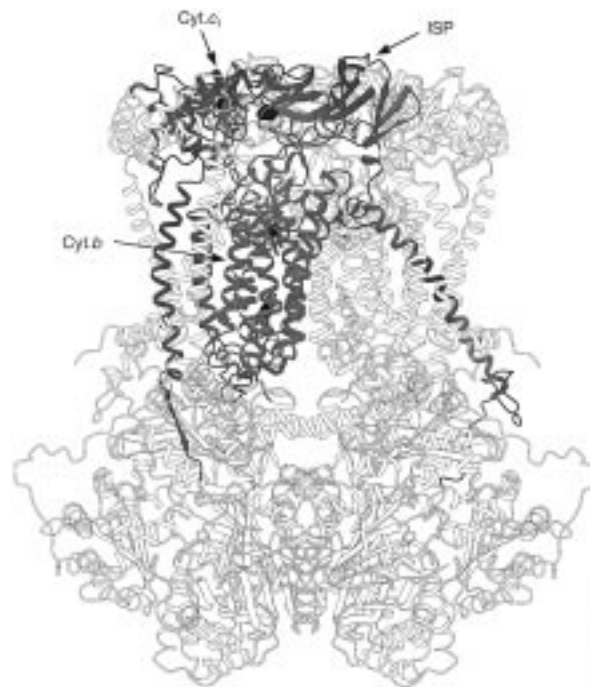

Fig. 1. The eleven-subunit structure of the complete cytochrome bc_1 complex from bovine heart mitochondria. One set of the functional unit including the Rieske [2Fe–2S] protein (ISP), cytochrome c_1, and cytochrome b is shown in dark grey.

STRUCTURE OF THE ISP EXTRINSIC DOMAIN

Before discussing details of the ISP conformational change, we would like to summarize the structure of the ISP extrinsic domain. The structure of domain has been determined as a water-soluble fragment, using the multiwavelength anomalous diffraction (MAD) technique, refined at 1.5 A resolution (Fig. 2; Iwata *et al.* 1996). The ISP extrinsic domain is a flat spherical molecule with dimensions of 45 × 40 × 25 A. The structure contains three layers of antiparallel β-sheets. Sheet 1 is formed by the strands β9, β10, and β1, sheet 2 by strands β2–β4, and sheet 3 by the strands β5–β8. An α-helix and a long loop are inserted between the strands β3 and β4. The three β-sheets can be represented by two β-sandwiches. One consists of sheets 1 and 2 and the other of sheets 2 and 3. The metal-binding site is at the top of the β-sandwich formed by the sheets 2 and 3. This cluster-binding fold can be separated from the rest of the structure (the base fold) and forms a small domainlike structure of its own. The cluster-binding and base folds are connected by an unusual intramolecular network of salt bridges and hydrogen bonds.

The [2Fe–2S] cluster is coordinated by two cysteine and two histidine side chains. The ligands coordinating the cluster originate from loops β4–β5 and β6–β7. Both loops contribute one cysteine and one
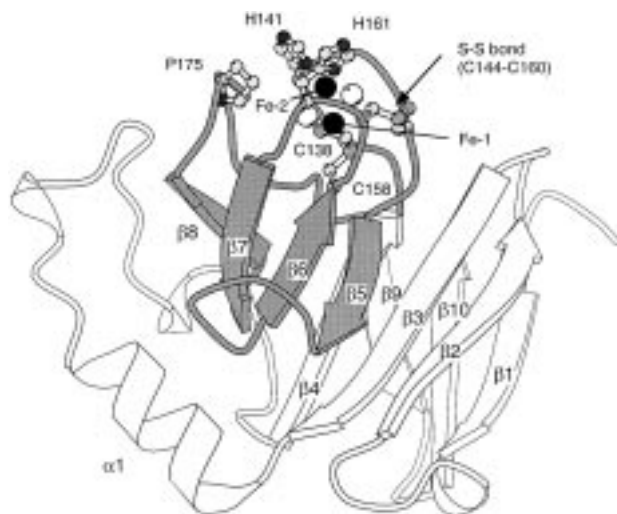

Fig. 2. Schematic ribbon diagram of the ISP extrinsic domain. Atoms in the iron–sulfur cluster (black, iron; white, sulfur), its ligands, the disulfide bond, and residue Pro175 are also shown. The secondary structures are labeled.

histidine residue each; loop β4–β5 contains Cys138 and His141 and loop β6–β7 contains Cys158 and His161. His141 and His161 are ligands for Fe–2, while Cys139 and Cys158 are ligands for Fe–1. Both loops (β4–β5 and β6–β7) contain an additional cysteine residue, Cys144 and Cys160; these cysteines form a disulfide bond connecting the two loops. A third loop following β8 covers the cluster from the other side. Mutations in this "*Pro* loop" contains the fully conserved sequence Gly174–Pro175–Ala176–Pro 177.

CONFORMATIONAL CHANGE OF THE ISP EXTRINSIC DOMAIN

As mentioned above, three different conformations of the ISP ("c_1", "*Int*" and "*b*" forms) have been reported (Fig. 3).

In the "c_1" form, the [2Fe–2S] cluster of the ISP is found very close to heme c_1 (Fig. 3A). The [2Fe–2S] cluster is only 15.5 A away from the Fe atom of heme c_1. The extrinsic domain of the ISP interacts with residues of the cytochrome c_1 subunit as well as loop ef of cytochrome *b*. Most of these interactions are van der Waals contacts and only two clear hydrogen bonds can be observed. One of them is formed between His161 of the ISP and a propionate group of heme c_1. All 127 Cα positions from the high resolution structure of the water-soluble ISP fragment (Iwata, *et al.* 1996) can be superimposed onto the ISP of our $P6_522$ form with an rms difference of 0.9 A. The main measurable difference is observed at strand β1 where the extrinsic domain is connected to the transmembrane anchor.

In the "*Int*" form, the [2Fe–2S] cluster of the ISP is found at a position closer to cytochrome *b* (Fig. 3B). The distances from the center of the [2Fe–2S] cluster of the ISP to the iron atoms of heme c_1 and heme b_L are 27.5 and 31 A, respectively. For the most part, residues in loop ef of cytochrome *b* form the binding site for the ISP extrinsic domain (Fig. 2B). There is no contact between the ISP and cytochrome c_1 in the "*Int*" form. The largest structural difference in cytochrome *b* between the "c_1" and the "*Int*" forms occur within loop ef. The average displacement of the loop is ca. 1 A with the largest deviation observed for residues Thr264 and Pro265. Notably, Pro265 is conserved in all known cytochrome *b* sequences. The contact region on the ISP is around a disulfide bond between Cys144 and Cys160. In this form, the closest distance between Q_P pocket and His161 of the ISP is
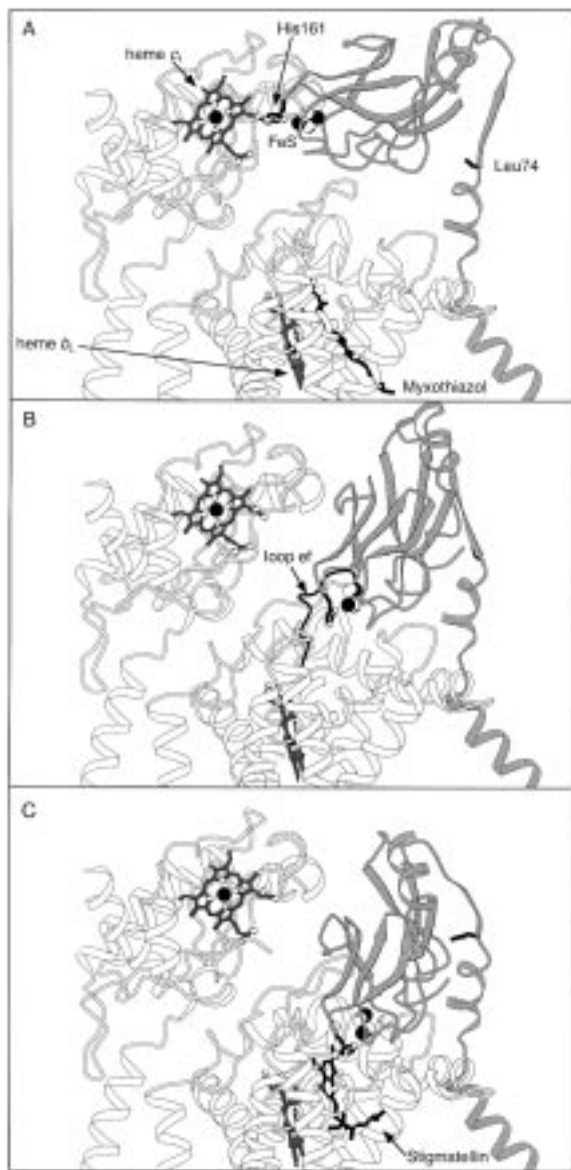
Fig. 3. Three different conformations of the "Rieske" protein (ISP) in relation to its neighbors. (A) Structure in the "c_1" form. An inhibitor myxothiazol, bound to the Q_P site, is also shown. (B) Structure in "Int" form. (C) Structure in the "b" form. An inhibitor stigmatellin, bound to the Q_P site, is also shown.

13 Å; therefore, it is impossible to form a hydrogen bond between His161 and a quinone or inhibitor in the Q_P pocket.

In the "b" form, the [2Fe–2S] cluster of the ISP is directly sitting on cytochrome b (Fig. 3C). The distances from the center of the [2Fe–2S] cluster to the iron atoms of heme c_1 and heme b_L are 31.6 and 26.4 Å, respectively (Zhang $et al.$, 1998; Crofts $et al.$, 1999).

The binding site for the ISP extrinsic domain is formed, largely, by residues in the horizontal helices αef and αcd2 and loops ef and gh of cytochrome b (Fig. 3C). This docking site is just above the Q_P binding pocket. In the structure, a hydrogen bond between His161 and inhibitor stigmatellin, located in the binding pocket, is observed (Zhang $et al.$, 1998; Crofts $et al.$, 1999). Except for this hydrogen bond, van der Waal interactions are dominant between ISP and cytochrome b.

The ISP structural differences found in the different crystal forms can be explained by two different motions: (1) a rotation of the entire ISP extrinsic domain and (2) a relative rotation between the cluster-binding fold and the base fold within the ISP extrinsic domain (Fig. 4). The rotation of the entire ISP extrinsic domain is clearly visible and has been well characterized using the three different forms. The motion within the ISP extrinsic domain is rather small, although this conformational change could be very important for the function (Iwata $et al.$, 1998). This motion was reported from the comparative study between the "c_1" and "Int" forms. However, for the "b" form of the bc_1 complex, the ISP water-soluble fragment structure was fitted as a rigid body due to the disorder of the electron density. Therefore, conformational changes within this domain have not been studied. For the "b" form, further investigations of these conformational changes are needed.

As a first approximation, the conformational change of the ISP is well explained by a rotation of the whole extrinsic domain. The motion from the "c_1" to "Int" position is approximately a 43 degrees rotation
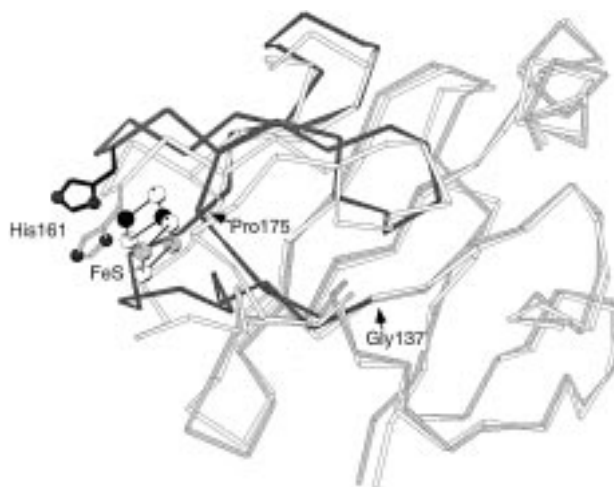

Fig. 4. Superimposing of the ISP extrinsic domains in the "c_1" and "Int" forms with the base fold. The "c_1" form is shown in white and the base and cluster binding folds of the "b" form is shown in grey and dark grey, respectively.

around the axis passing near Leu74 at the carboxy-terminal end of the short helix $\alpha0'$. This transformation includes only a 0.24 A translation along the rotation axis, and is thus well simulated by a single rotation. At the carboxy-terminal end of the helix $\alpha0'$, a clear conformational change in the polypeptide main chain is observed. A hydrogen bond between Leu69 O and the Ser72 N is present in the "c_1" form, which induces a 3_{10}-helix conformation, but not in the "Int" form, where the 3_{10}-helix is absent.

The motion from the "Int" to "b" position is approximately a 33 degrees rotation around the axis passing near Gly137, which exist at the interface between the metal cluster binding and base folds of the ISP extrinsic domain. A screw component along the rotation axis is as small as 0.48 A, and, therefore, this transformation could also be fit with a single rotation model. Since the structure of the "b" form ISP is fitted as a rigid body, atomic details of this conformational change is unclear. The conformational changes of the ISP are not only due to a rotation at the end of the $\alpha0'$, but also a rotation within the ISP extrinsic domain looks to be involved.

Interestingly, the directions of the two rotations, from "c_1" to "Int" positions and from "Int" to "b" positions, are totally different. The angle of the two rotation axes is as large as 65 degrees. If we force to connect the "c_1" and "b" positions by a single rotation, the rotation angle is calculated as 64 degrees; however, this transformation contains 2.8 A translation along the rotation axis, and, therefore, can not be well fitted by a single rotation. The motion of the ISP extrinsic domain is better explained by a combination of two rotations.

This "kink" of the ISP trajectory is due to a collision with loop ef of cytochrome b and the ISP. If the "c_1" and "b" positions are connected by a single rotation, the ISP extrinsic domain severely clashes with loop ef during the rotation. In order to accomplish this, a movement greater than 3 A of loop ef must occur in order for the ISP to pass through. To avoid this energetically unfavorable collision, the ISP needs to go around loop ef. The turning point of this detour is observed as the "Int" position. This stable "Int" position may have a physiological importance, since a mutation of Thr265 in loop ef leads to severe loss of the quinol oxidation activity (Brandt, 1998).

Conformational differences within the ISP extrinsic domain between the "c_1" and the "Int" forms are rather small but are nonetheless significant. As mentioned above, the ISP extrinsic domain has two separate folds (Fig. 2); The metal cluster-binding fold (residues 137–181) and the base fold (residues 74–136 and 182–196, Iwata *et al.*, 1996). A clear positional displacement between these two folds is observed between the "c_1" and the "Int" forms (Fig. 4). The structure of the ISP subunit for the "c_1" form is the same as that of the water-soluble ISP fragment. However, in the "Int" form, the cluster-binding fold appears to be detached from the base fold into an "open" conformation. When the extrinsic domains of the two crystal forms are superimposed using the base fold residues, the rms difference for the Cα positions in the cluster binding fold is 1.6 A. In the "Int" form, the salt bridge Asp109–Arg170 as well as the associated hydrogen bond network between the cluster-binding fold and the base fold, which connects these two structures in the "c_1" form, are absent. As a result, the gap between the two folds becomes more exposed to the solvent region. In addition, the large conformational change at Gly174–Pro175 has been observed between the two forms. Pro175 in the "Int" form shows a better fit with a *cis*-proline conformation instead of a *trans*-proline that is observed in both the "c_1" form as well as the water-soluble ISP fragment. It should be noted that *cis*-Pro175 is found in the structure of the water-soluble Rieske fragment from the b_6f complex, which is a counterpart of the bc_1 complex in chloroplast (Carrell *et al.* 1997).

IMPLICATIONS FOR A THREE-STATE MECHANISM OF HYDROQUINONE OXIDATION

It is generally accepted that the electron transfer is coupled to proton translocation by the protonmotive Q-cycle mechanism first proposed by Peter Mitchell (Brandt and Trumpower, 1994; Mitchell, 1976). The central reaction of the Q cycle is a bifurcation of the pathway of electrons upon oxidation of hydroquinone at the Q_P site. During the hydroquinone oxidation reaction, the first electron is always transferred to the ISP cluster and the second electron to heme b_L. This electron bifurcation can be well explained using the motion of the ISP extrinsic domain (Croft *et al.*, 1999; Zhang *et al.*, 1998; Iwata *et al.*, 1998). To make a mechanistic model of the hydroquinone oxidation at the Q_P-binding site using the ISP motion, we need to consider the following observations.

i. The oxidized [2Fe–2S] cluster is not hydrogen bonded to other subunits. The "Int" position looks

suitable for the oxidized cluster, as it has been shown that the oxidized [2Fe–2S] cluster is not involved in hydrogen bonding in the bc_1 complex (Link *et al.*, 1997). Without a hydrogen bond at His161, the oxidized ISP is most likely oscillating around the "*Int*" position (Fig. 5A).

ii. The ISP should occupy the "*b*" position when the [2Fe–2S] cluster interacts with QH$^-$ or QH$\cdot$ From the study using the inhibitor stigmatellin, it is assumed that a direct hydrogen bond is formed between the ISP and QH$^-$ or QH$\cdot$ during the electron transfer (Lancaster and Michel, 1997; Robertson *et al.* 1990; von Jagow and Ohnishi, 1985). This is only possible in the "*b*" form, as it is confined by geometry (Fig. 5A).

iii. The reduced [2Fe–2S] cluster preferentially occupies the "c_1" positional state when QH$^-$ or QH$\cdot$ is not present in the Q_P pocket. If the Q_P site is blocked by a methoxyacrylate inhibitor, which can not form hydrogen bonds with the ISP, it has been reported that the reduced [2Fe–2S] stays away from cytochrome *b*, but still forms a hydrogen bond with something else (Brandt and von Jagow, 1991; Brandt U *et al.*, 1991). This suggests that the ISP extrinsic domain stays in the "c_1" position, where a hydrogen bond formed with a propionate from the heme (Fig. 5A).

To encompass the above observation, we propose the following mechanistic model of the hydroquinone oxidation cycle, known as the "three-state model" (Iwata *et al.*, 1998) that is described as follows using Fig. 5B.

Before the substrate binds, the oxidized ISP is in the "*Int*" position (*a*). Without a hydrogen bond at His161, the oxidized ISP is most likely oscillating around the "*Int*" position. Hydroquinone will bind in the quinone-binding site of cytochrome *b* (*b*). Before hydroquinone can be oxidized, it is assumed to be deprotonated; this deprotonation represents the activation barrier of hydroquinone oxidation (Brandt and Okun, 1997). The interaction with the deprotonated hydroquinone (QH$^-$) will move the ISP toward the "*b*" position (*c*). After the electron transfer, the resulting semiquinone is tightly bound to the reduced [2Fe–2S] cluster at the "*b*" position and stabilized (*d*; Link *et al.*, 1997). After the second electron transfer from semiquinone to heme b_L, the interaction between the [2Fe–2S] cluster and the resulting quinone is weakened so that the reduced ISP can now occupy the preferred "c_1" position (*e*), which allows rapid electron transfer from the [2Fe–2S] cluster to heme c_1. Finally, when the electrons have been transferred to cyto-
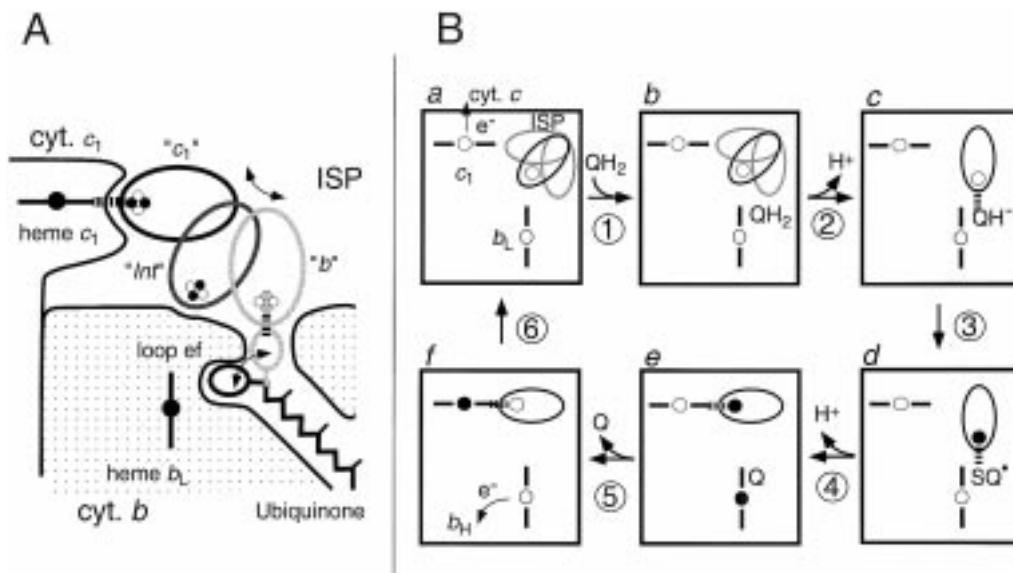

Fig. 5. (A) A schematic drawing of the different positions of the ISP extrinsic domain. Dotted lines indicate hydrogen bonds formed by the [2Fe–2S] cluster. (B) "Three-state model" of the hydroquinone oxidation in the Q_P site of the bc_1 complex based on the switching of the Rieske protein between the "*Int*" position (*a, b*), the "*b*" position (*c, d*), and the "c_1" position (*e, f*). Filled circles are reduced reduced [2Fe–2S] cluster; empty circles are oxidized reduced [2Fe–2S] cluster. Dotted lines indicate hydrogen bonds formed by the reduced [2Fe–2S] cluster. See text for details.

chrome c and to heme b_H, the ISP can go back to its initial "*Int*" position and the site is ready for the next reaction cycle. This reaction mechanism combines the evidence from the present X-ray structures with elements of the "affinity-change mechanism" (Link *et al.*, 1997) and of the "catalytic-switch mechanism" (Brandt and von Jagow, 1991; Brandt *et al.*, 1991); it is fully compatible with all biochemical observations and explains the bifurcation of the electron pathways as well as the mode of action of the inhibitors of the bc_1 complex. All electron transfer reactions occur between species when they are hydrogen bonded to each other; therefore, electron transfer will be extremely rapid and most likely not rate limiting.

ACKNOWLEDGMENT

REFERENCES

Brandt, U., and von Jagow, G. (1991). *Eur. J. Biochem.* **195**, 163–170.

Brandt, U., Haase, U., Schagger, H., and von Jagow, G. (1991). *J. Biol. Chem.* **266**, 19958–19964.

Brandt, U., and Okun, J. (1997). *Biochemistry* **36**, 11234–11240.

Brandt, U. (1998). *Biochim. Biophys. Acta* **1365**, 261–268.

Brandt, U., and Trumpower, B. (1994). *Crit. Rev. Biochem. Mol. Biol.* **29**, 165–197.

Carrell, C. J., Zhang, H., Cramer, W. A., and Smith, J. L. (1997). *Structure* **5**, 1613–1625.

Crofts, A. R., Barquera, B., Gennis, R. B., Kuras, R., Guergova-Kuras, M., and Berry, E. A. (1999). In *The Phototrophic Prokaryotes* (Peschek, G.A., Loeffelhardt, W., and Schmetterer, G., eds.), Plenum, New York, pp. 229–239. (This paper was submitted at the IXth International Symposium on Phototrophic Prokaryotes, Vienna, Sept. 1997. Publication was delayed until Jan. 1999.)

Iwata, S., Saynovits, M., Link, T. A., and Michel, H. (1996). *Structure* **4**, 567–579.

Iwata, S., Lee, J. W., Okada, K., Lee, J. K., Iwata, M., Rasmussen, B., Link, T. A., Ramaswamy, S., and Jap, B. K. (1998). *Science* **281**, 64–71.

Kim, H., Xia, D., Yu, C.-A., Xia, J.-Z., Kachurin, A. M., Zhang, L., Yu, L., and Deisenhofer, J. (1998). *Proc. Natl. Acad. Sci. U.S.* **95**, 8026–8033.

Lancaster, C. R. D., and Michel, H. (1997). *Structure* **5**, 1339–1359.

Link, T. A. (1997). *FEBS Lett.* **412**, 257–264.

Link, T. A., Hatzfeld, O. M., and Saynovits, M. (1997). In *Bioinorganic Chemistry.Transition Metals in Biology and Their Coordination Chemistry* (Trautwein, A. X., ed.), Wiley-VCH, Weinheim, pp. 00–00.

Mitchell, P. (1976). *J. Theoret. Biol.* **62**, 327–367.

Robertson, D. E., Daldal, F., and Dutton P. L. (1990). *Biochemistry* **29**, 11249–11260.

Robertson, D. E., Ding, H., Chelminski, P. R., Slaughter, C., Hsu, J., Moomaw, C., Tokito, M., Daldal, F., and Dutton, P. L. (1993). *Biochemistry* **32**, 1310–1317.

von Jagow, G., and Ohnishi, T. (1985). *FEBS Lett.* **185**, 311–315.

Xia, D., Yu, C.-A., Kim, H., Xia, J.-Z., Kachurin, A. M., Zhang, L., Yu, L., and Deisenhofer, J. (1997). *Science* **277**, 60–66.

Yang, X. H., and Trumpower, B. L. (1986). *J. Biol. Chem.* **261**, 12282–12289.

Zhang, Z., Huang, L., Shulmeister, V. M., Chi, Y.-I., Kim, K.-K., Hung, L.-W., Crofts, A. R., Berry, E. A., and Kim, S.-H. (1998). *Nature* **392**, 677–687.